SUPPLEMENTARY MATERIAL

Comparative kinetic analysis of redox flow battery electrolytes: from micro-fibers to macro-felts

Vincent Feynerol[a], Ranine El Hage[a], Mariela Brites Helú[a], Vanessa Fierro[b], Alain Celzard[b], Liang Liu[a], Mathieu Etienne[a]

[a]*Laboratoire de Chimie Physique et Microbiologie pour les Matériaux et l'Environnement (LCPME), UMR 7564, CNRS-Université de Lorraine*
405 Rue de Vandoeuvre, 54600 Villers-lès-Nancy, France
[b]*Institut Jean Lamour, UMR 7198 CNRS - Université de Lorraine ENSTIB*
27 rue Philippe Seguin BP 1041, F-88051 EPINAL Cedex 9, France
vincent.feynerol@univ-lorraine.fr

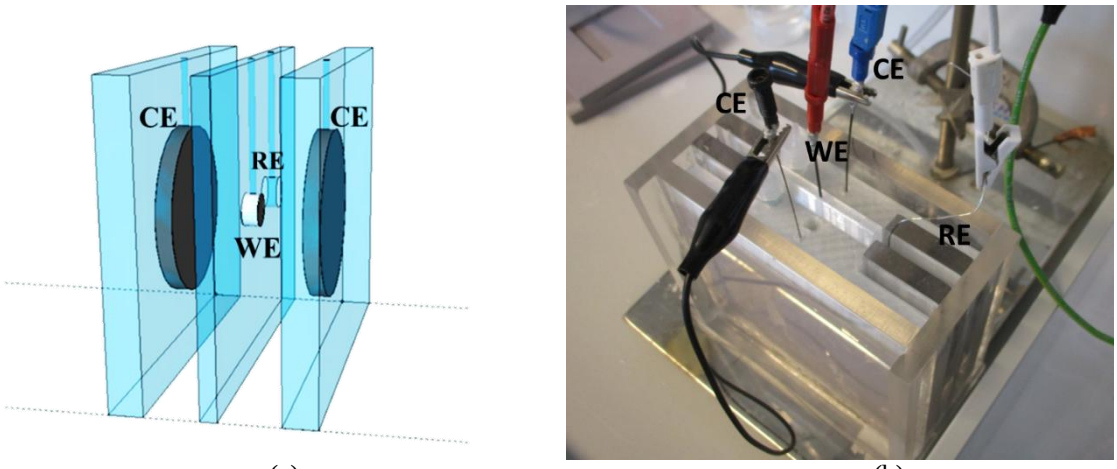

(a) (b)

Figure S1*: (a) 3D sketch and (b) photograph of the electrolysis cell for experiments with graphite felts*

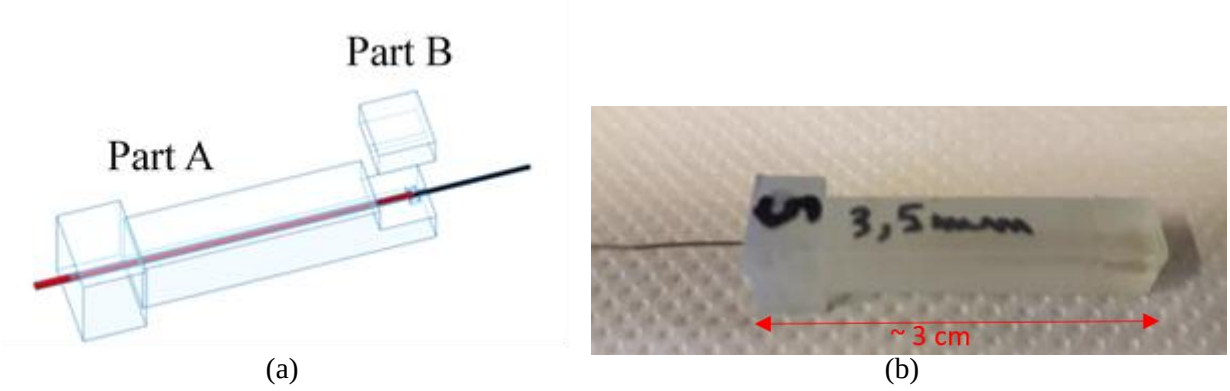

(a) (b)

(c)

Figure S2: (a) Sketch of the microelectrode support : the red piece represents the copper wire while the black one is the carbon fibre *(b) Photograph of a microelectrode carbon fibre (the fibre being located on the right-side and the connecting wire to the left side) and (c) optical microscope view of the carbon fibre.*

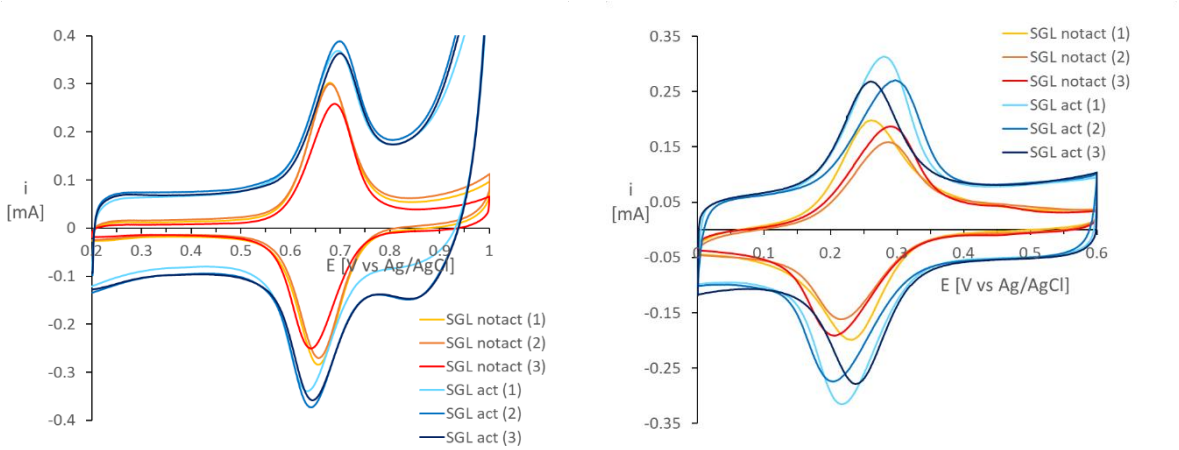

(a) TEMPO-based (b) $(NH_4)_4Fe(CN)_6$

Figure S3: *Cyclic voltammograms for the different replication*

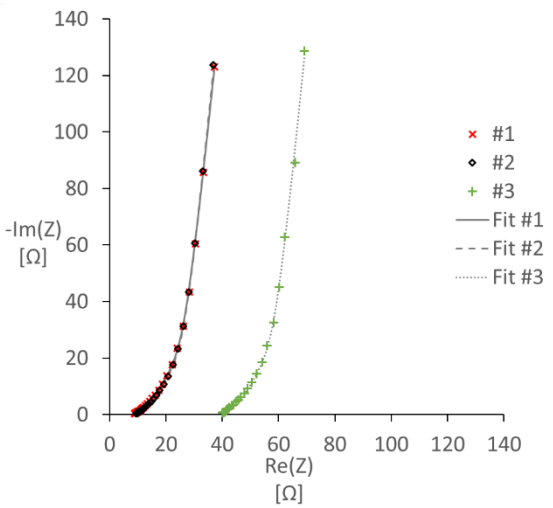

a. TEMPO-based on SGL not activated

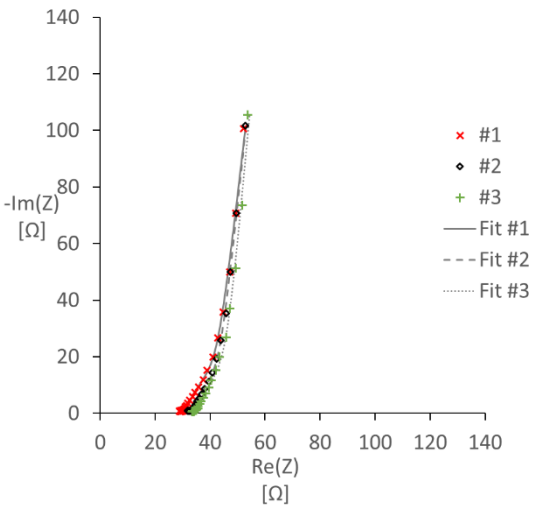

b. TEMPO-based on SGL activated

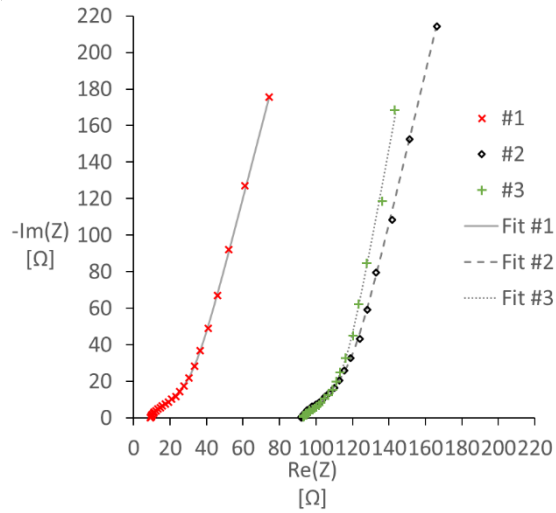

c. $(NH_4)_4Fe(CN)_6$ on SGL not activated

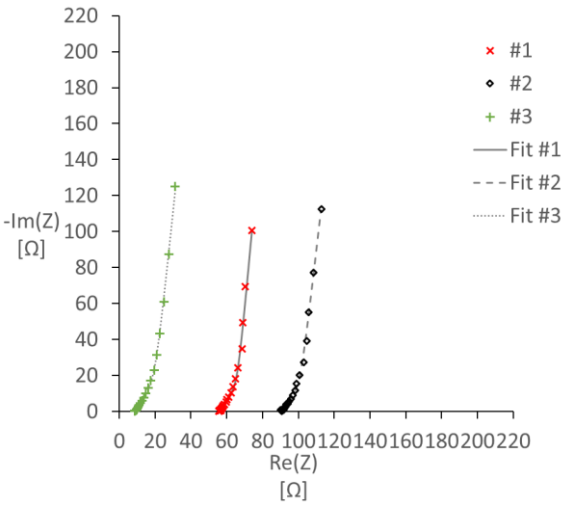

d. $(NH_4)_4Fe(CN)_6$ on SGL activated

***Figure S4**: Experimental Nyquist diagrams and their fits for all replications with porous graphite felts*

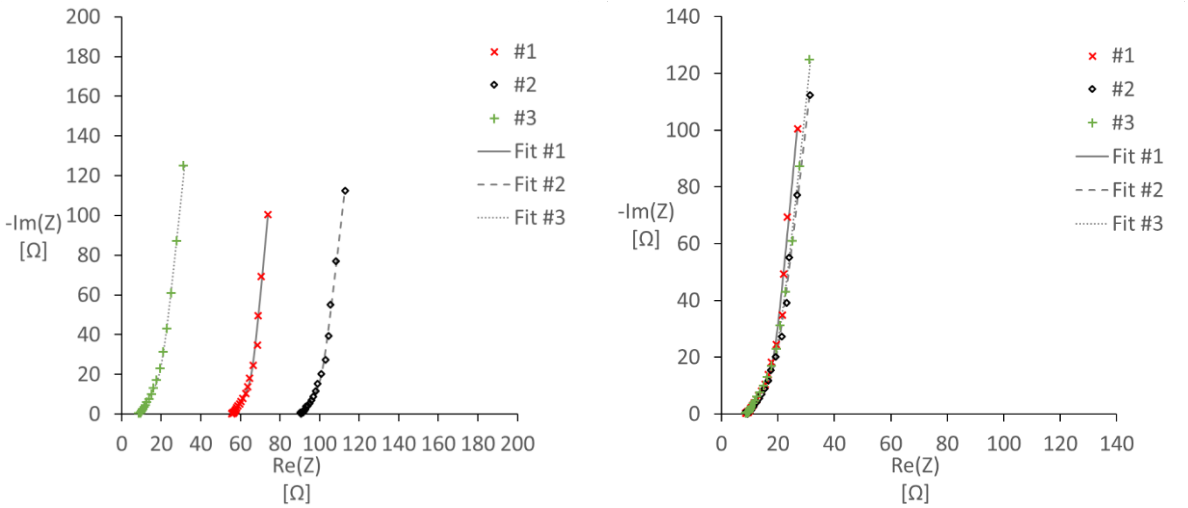

(a) Before translation of Re(Z) part (b) After translation of Re(Z) part

***Figure S5**: Nyquist diagram at formal potential for the different replication of $(NH_4)_4Fe(CN)_6$ EIS measurement on SGL carbon felt (activated). Before and after translating the real part for d.c. resistance of all curves to match.*

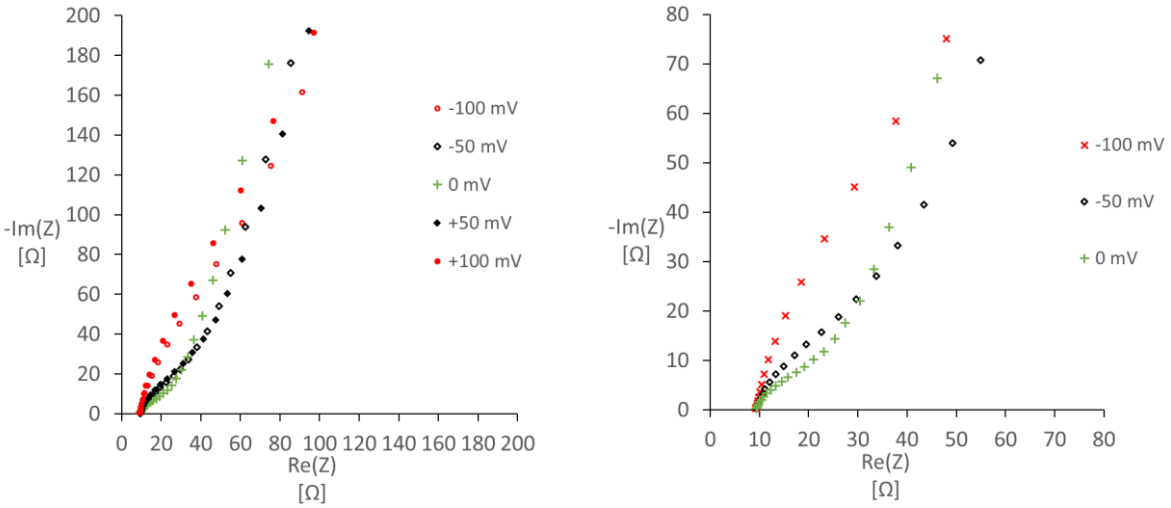

***Figure S6**: Nyquist diagram at different (E- E^{0}') where E is the potential and E^{0}' is estimated formal potential, for one of the replications of $(NH_4)_4Fe(CN)_6$ EIS measurement on SGL carbon felt (non-activated)*

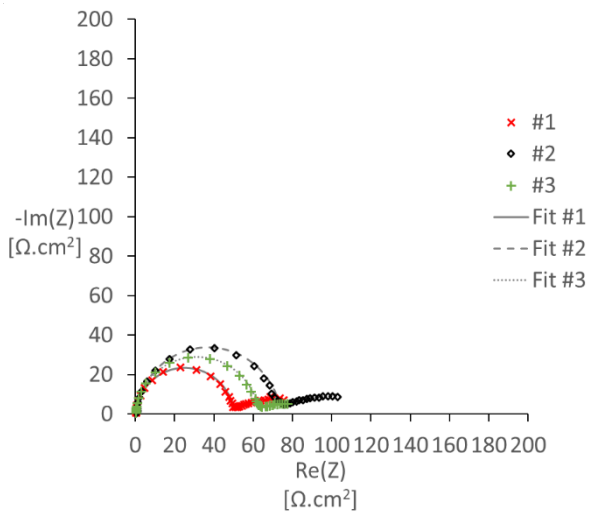

a. TEMPO-based on SGL not activated

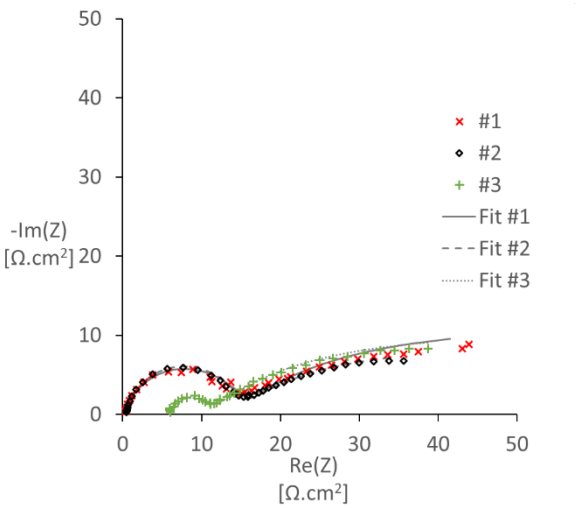

b. TEMPO-based on SGL activated

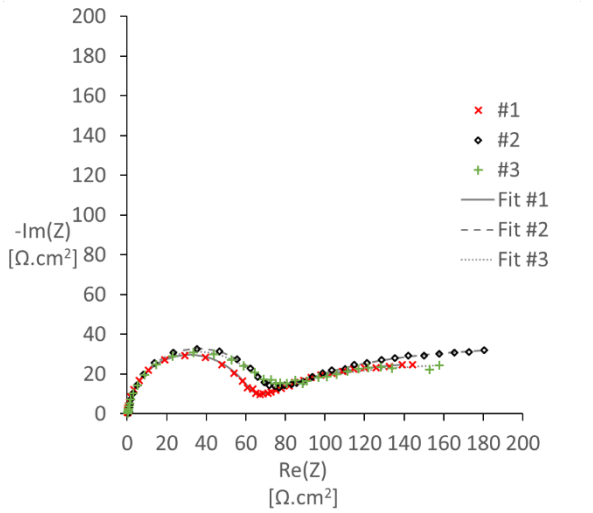

c. $(NH_4)_4Fe(CN)_6$ on SGL not activated

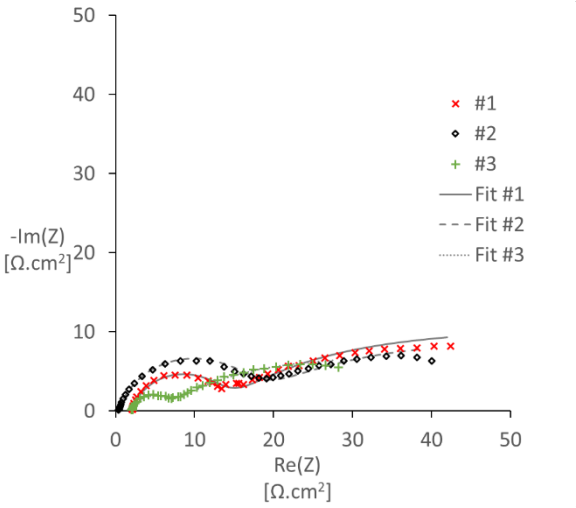

d. $(NH_4)_4Fe(CN)_6$ on SGL activated

***Figure S7**: Experimental Nyquist diagrams and their fits for all replications with carbon fibre microelectrodes*

***Table S1**: Optimized parameters' values for each replication and their average and standard deviation values for EIS experiments carried out on **non-activated** SGL carbon felt with TEMPO-based molecule at estimated formal potential of 0.66 V vs Ag/AgCl QRE.*

		TEMPO-based				
		SGL GFD 4.6 n.a.				
		#1	#2	#3	**Average**	Std Dev
R_{ohm}	[Ω]	8.7	9.2	39.5	**19.1**	17.7
C	[F cm^{-2} $s^{\gamma-1}$]	1.05E-04	1.03E-04	9.83E-05	**1.02E-04**	3.51E-06
γ	[-]	0.97	0.97	0.97	**0.97**	0.002
k^0	[cm s^{-1}]	1.62E-03	1.61E-03	1.49E-03	**1.57E-03**	7.26E-05
l_p	[cm]	0.0011	0.0011	0.0010	**0.0011**	0.00003
S_c	[cm^2 cm^{-3}]	327.2	333.3	334.9	**331.8**	4.1
f_p	[-]	2.93	2.83	3.28	**3.01**	0.24
φ	[-]	0.91*	0.91*	0.91*	**0.91***	0.00

*value fixed during optimization

***Table S2**: Optimized parameters' values for each replication and their average and standard deviation values for EIS experiments carried out on **activated** SGL carbon felt with TEMPO-based molecule at estimated formal potential of 0.66 V vs Ag/AgCl QRE.*

		TEMPO-based				
		SGL GFD 4.6 act				
		#1	#2	#3	**Average**	Std Dev
R_{ohm}	[Ω]	28.5	31.7	33.1	**31.1**	2.3
C	[F cm^{-2} $s^{\gamma-1}$]	8.55E-05	9.05E-05	1.11E-04	**9.56E-05**	1.34E-05
γ	[-]	1.00	0.99	0.99	**0.99**	0.01
k^0	[cm s^{-1}]	1.22E-02	8.59E-02	7.48E-02	**5.77E-02**	3.97E-02
l_p	[cm]	0.0020	0.0020	0.0021	**0.0020**	0.0001
S_c	[cm^2 cm^{-3}]	303.8	295.6	259.8	**286.4**	23.4
f_p	[-]	1.32	1.10	1.20	**1.21**	0.11
φ	[-]	0.90*	0.91*	0.92*	**0.91***	0.01

*value fixed during optimization

***Table S3**: Optimized parameters' values for each replication and their average and standard deviation values for EIS experiments carried out on **non-activated** SGL carbon felt with ammonium hexacyanoferrate at estimated formal potential of 0.25 V vs Ag/AgCl QRE.*

		$(NH_4)_4Fe(CN)_6$				
		SGL GFD 4.6 n.a.				
		#1	#2	#3	**Average**	Std Dev
R_{ohm}	[Ω]	8.3	91.1	92.5	**64.0**	48.2
C	[F cm^{-2} $s^{\gamma-1}$]	5.38E-05	4.49E-05	5.95E-05	**5.27E-05**	7.34E-06
γ	[-]	1.00*	1.00*	1.00*	**1.00**	0.00
k^0	[cm s^{-1}]	2.60E-03	1.87E-03	2.14E-03	**2.20E-03**	3.70E-04
l_p	[cm]	0.0010	0.0008	0.0010	**0.0010**	0.00009
S_c	[cm^2 cm^{-3}]	289.3	288.8	305.7	**294.6**	9.6
f_p	[-]	6.70	7.15	5.47	**6.44**	0.87
φ	[-]	0.79	0.81	0.84	**0.81**	0.02

*value fixed during optimization

***Table S4**: Optimized parameters' values for each replication and their average and standard deviation values for EIS experiments carried out on **activated** SGL carbon felt with ammonium hexacyanoferrate at estimated formal potential of 0.25 V vs Ag/AgCl QRE.*

		$(NH_4)_4Fe(CN)_6$				
		SGL GFD 4.6 act				
		#1	#2	#3	**Average**	Std Dev
R_{ohm}	[Ω]	55.3	90.0	8.2	**51.2**	41.1
C	[F cm^{-2} $s^{\gamma-1}$]	9.15E-05	8.79E-05	9.19E-05	**9.04E-05**	2.21E-06
γ	[-]	1.00	0.99	0.99	**1.00**	0.00
k^0	[cm s^{-1}]	1.21E-02	5.69E-02	2.91E-02	**3.27E-02**	2.26E-02
l_p	[cm]	0.0018	0.0019	0.0019	**0.0019**	0.00004
S_c	[cm^2 cm^{-3}]	314.6	276.4	243.3	**278.1**	35.7
f_p	[-]	1.29	1.53	1.11	**1.31**	0.21
φ	[-]	0.92*	0.90*	0.91*	**0.91***	0.01

*value fixed during optimization

***Table S5**: Optimized parameters' values for each replication and their average and standard deviation values for EIS experiments carried out on carbon fibre microelectrode drawn from **non-activated** SGL carbon felt with TEMPO-based molecule at estimated formal potential of 0.66 V vs Ag/AgCl QRE.*

		TEMPO-based				
		SGL GFD 4.6 n.a.				
		#1	#2	#3	Average	Std Dev
R_{ohm}	[Ω]	387.5	723.9	491.6	**534.4**	172.2
Y_0	[$F.cm^{-2}.s^{\gamma-1}$]	2.48E-06	2.30E-06	3.26E-06	**2.68E-06**	5.10E-07
γ	[-]	0.97	0.96	0.96	**0.96**	0.01
k^0	[$cm\ s^{-1}$]	1.09E-03	7.42E-04	8.68E-04	**9.00E-04**	1.75E-04
D	[$cm^2\ s^{-1}$]	3.98E-06	3.33E-06	6.09E-06	**4.47E-06**	1.44E-06

***Table S6**: Optimized parameters' values for each replication and their average and standard deviation values for EIS experiments carried out on carbon fibre microelectrode drawn from **activated** SGL carbon felt with TEMPO-based molecule at estimated formal potential of 0.66 V vs Ag/AgCl QRE.*

		TEMPO-based				
		SGL GFD 4.6 act				
		#1	#2	#3	**Average**	Std Dev
R_{ohm}	[Ω]	399.2	496.8	6918.9	**2605.0**	3736.3
Y_0	[$F\ cm^{-2}\ s^{\gamma-1}$]	2.18E-05	1.20E-05	4.29E-05	**2.56E-05**	1.58E-05
γ	[-]	0.83	0.89	0.80	**0.84**	0.04
k^0	[$cm\ s^{-1}$]	3.66E-03	3.76E-03	1.00E-02	**5.81E-03**	3.63E-03
D	[$cm^2\ s^{-1}$]	3.43E-06	4.50E-06	3.70E-06	**3.88E-06**	5.59E-07

***Table S7**: Optimized parameters' values for each replication and their average and standard deviation values for EIS experiments carried out on carbon fibre microelectrode drawn from **non-activated** SGL carbon felt with ammonium hexacyanoferrate at a potential of 0.6 V vs Ag/AgCl QRE.*

		$(NH_4)_4Fe(CN)_6$				
		SGL GFD 4.6 n.a.				
		#1	#2	#3	**Average**	Std Dev
R_{ohm}	[Ω]	373.6	747.1	586.2	**569.0**	187.4
Y_0	[F cm^{-2} $s^{\gamma-1}$]	2.63E-06	2.28E-06	5.99E-06	**3.64E-06**	2.05E-06
γ	[-]	0.97	0.97	0.95	**0.96**	0.02
k^0	[cm s^{-1}]	1.05E-05	1.91E-05	2.31E-05	**1.76E-05**	6.44E-06
D	[cm^2 s^{-1}]	7.47E-06	1.19E-05	1.86E-05	**1.26E-05**	5.58E-06
m_O	[cm s^{-1}]	9.82E-04	8.50E-04	1.18E-03	**1.00E-03**	1.63E-04

***Table S8**: Optimized parameters' values for each replication and their average and standard deviation values for EIS experiments carried out on carbon fibre microelectrode drawn from **activated** SGL carbon felt with ammonium hexacyanoferrate at estimated formal potential of 0.25 V vs Ag/AgCl QRE.*

		$(NH_4)_4$ $Fe(CN)_6$				
		SGL GFD 4.6 act				
		#1	#2	#3	**Average**	Std Dev
R_{ohm}	[Ω]	2379.8	410.6	3480.9	**2090.4**	1555.5
Y_0	[F cm^{-2} $s^{\gamma-1}$]	6.09E-05	9.23E-05	1.70E-04	**1.08E-04**	5.63E-05
γ	[-]	0.82	0.80	0.77	**0.79**	0.02
k^0	[cm s^{-1}]	4.48E-03	3.06E-03	1.03E-02	**5.95E-03**	3.84E-03
D	[cm^2 s^{-1}]	3.60E-06	4.15E-06	5.39E-06	**4.38E-06**	9.17E-07

***Table S9**: Input parameters kept constant for the simulation of Cyclic Voltammetry in Polarographica*

Parameters symbols and units	Values
n [-]	1
α [-]	0.5
T [°C]	25
Scan rate [mV s^{-1}]	10
c [mol L^{-1}]	10^{-4}
D [cm^2 s^{-1}]	3.8 10^{-6}
$E^{0'}$ [V vs ref]	0.25
R_{Ohm} [Ω]	10
Intervals of distribution function [-]	10
Cylinders per mm² [-]	722
Carbon fibre radius [µm]	4.5

Expression of Paasch, Micka and Gersdorf model as a function of formal potential

Defining the electrode potential *E* (Defined as $\tilde{E}$ in the original paper*)* within porous electrode as the difference between solid phase electrical potential ϕ_1 and liquid phase electrical potential ϕ_2, and starting with equation (2) from Paasch, Micka and Gersdorf paper [15]. Convention for the sign of the current was kept American (positive current for reduction) in order to limit possible confusion.

$$E = \phi_1 - \phi_2 d \tag{S.1}$$

$$AS_c C\frac{\partial E}{\partial t} = -\frac{A}{\rho_2}\frac{\partial^2 \phi_2}{\partial x^2} + AS_c nFk^0 C_O^{*1-\alpha} C_R^{*\alpha}\left[e^{-\frac{\alpha nF}{R_g T}(E-E_n)} - e^{\frac{(1-\alpha)nF}{R_g T}(E-E_n)}\right] \tag{S.2}$$

Butler-Volmer contribution to the equation can be replaced with classic i-E expression as a function of formal potential $E^{0\prime}$ and surface concentrations:

$$AS_c C\frac{\partial E}{\partial t} = -\frac{A}{\rho_2}\frac{\partial^2 \phi_2}{\partial x^2} + AS_c nFk^0\left[C_O^s e^{-\frac{\alpha nF}{R_g T}\left(E-E^{0\prime}\right)} - C_R^s e^{\frac{(1-\alpha)nF}{R_g T}\left(E-E^{0\prime}\right)}\right] \tag{S.3}$$

Applied potential during impedance measurement can be expressed as a function of the average potential $\bar{E}$ around which oscillation with time ΔE:

$$E = \bar{E} + \Delta E \tag{S.4}$$

Equation (S.3) can therefore be rearranged as:

$$AS_c C\frac{\partial \Delta E}{\partial t} = -\frac{A}{\rho_2}\frac{\partial^2 \phi_2}{\partial x^2} + AS_c nFk^0\left[M_O e^{-\frac{\alpha nF}{R_g T}\Delta E} - M_R e^{\frac{(1-\alpha)nF}{R_g T}\Delta E}\right] \tag{S.5}$$

Where the expressions of M_O and M_R are given below:

$$M_O = C_O^s \exp\left(-\alpha \frac{nF}{R_g T}\left(\bar{E} - E^{0'}\right)\right) \quad \textbf{(S.6)}$$

$$M_R = C_R^s \exp\left((1-\alpha) \frac{nF}{R_g T}\left(\bar{E} - E^{0'}\right)\right) \quad \textbf{(S.7)}$$

The classic assumption of small amplitudes allows to linearize the exponential terms with a first order Taylor expansion:

$$AS_c C \frac{\partial \Delta E}{\partial t} = -\frac{A}{\rho_2}\frac{\partial^2 \phi_2}{\partial x^2} - \frac{AS_c n^2 F^2 k^0}{R_g T}[\alpha M_O + (1-\alpha) M_R]\Delta E + AS_c nF k^0 (M_O - M_R) \quad \textbf{(S.8)}$$

Assuming a Nernstian system and substituting surface concentrations with their expressions according to Nernst equation given in **equations (8)** and **(9)** (in the paper) allows to further elucidate M_O and M_R:

$$M_O = (C_O^* + C_R^*) \cdot \frac{\exp\left((1-\alpha)\frac{nF}{R_g T}\left(\bar{E} - E^{0'}\right)\right)}{1 + \exp\left(\frac{nF}{R_g T}\left(\bar{E} - E^{0'}\right)\right)} = M_R \quad \textbf{(S.9)}$$

Hence in the case where surface concentrations are assumed to be equal to Nernst concentrations, M_O is equal to M_R, simplifying **equation (S.8)** into **equation (S.10)**:

$$AS_c C \frac{\partial \Delta E}{\partial t} = -\frac{A}{\rho_2}\frac{\partial^2 \phi_2}{\partial x^2} - \frac{AS_c n^2 F^2 k^0 (C_O^* + C_R^*) e^{\frac{(1-\alpha)nF}{R_g T}\left(\bar{E} - E^{0'}\right)}}{R_g T\left(1 + e^{\frac{nF}{R_g T}\left(\bar{E} - E^{0'}\right)}\right)} \cdot \Delta E \quad \textbf{(S.10)}$$

Although this equation might seem complicated, it is virtually the same equation as equation (9) from the original paper, with exchange current density replaced by M_R which depends on available parameters. Symmetrically a similar development is made for equation (10) from Paasch team's original paper, and their equation (11) is obtained, only with a new expression for *k* which was presented here in **equation (4)** of our paper. Integration of this equation strictly gives the same analytical solution for complex impedance, but with a different value for *k*.

Development of quasi-reversible model

General expression of Fick's second law of diffusion for species O (the oxidant) is:

$$\frac{\partial C_O}{\partial t} = D_O \nabla^2 C_O \qquad \textbf{(S.11)}$$

In cylindrical geometry for an infinitely long cylinder and under steady state assumption, this equation resumes to:

$$\frac{d^2 C_O}{dr^2} = -\frac{1}{r} \cdot \frac{dC_O}{dr} \qquad \textbf{(S.12)}$$

This differential equation can be solved taking, as first boundary condition the flux continuity at the electrode surface using Faraday's law, and as second boundary condition the concentration equal to bulk electrolyte concentration at a distance δ of the electrode's walls (finite diffusion). The solution is as follows[36]:

$$C_O(r) = C_O^* + \frac{r_0 I_{ss}}{nFAD_O} \ln\left(\frac{\delta}{r}\right) \qquad \textbf{(S.13)}$$

This solution is true for a radius comprised between electrode's radius r_0 and Nernst diffusion layer δ. Surface concentration is obtained for $r = r_0$:

$$C_O^s = C_O^* + \frac{r_0 I_{ss}}{nFAD_O} \ln\left(\frac{\delta}{r_0}\right) \qquad \textbf{(S.14)}$$

And similarly, for the reductant R:

$$C_R^s = C_R^* - \frac{r_0 I_{ss}}{nFAD_R} \ln\left(\frac{\delta}{r_0}\right) \qquad \textbf{(S.15)}$$

Assuming the same value of diffusion coefficient for O and R, one may identify mass transfer coefficient m_O:

$$m_O = \frac{D}{r_0 \ln\left(\frac{\delta}{r_0}\right)} \qquad \textbf{(S.16)}$$

Surface concentration expressions may then be substituted in classic i-E expression, just as Bard and Faulkner demonstrated for planar diffusion [31]:

$$I_{ss} = nFAk^0 \left[\left(C_R^* - \frac{I_{ss}}{m_O} \right) \exp\left(\frac{(1-\alpha)nF}{R_g T} (E - E^{0\prime}) \right) - \left(C_O^* + \frac{I_{ss}}{m_O} \right) \exp\left(-\frac{\alpha nF}{R_g T} (E - E^{0\prime}) \right) \right] \quad \textbf{(S.17)}$$

Rearranging this equation permits obtaining an i-E relation as a function of bulk electrolyte concentrations:

$$I_{ss} = \frac{nFAk_0 \left[C_R^* e^{\frac{(1-\alpha)nF}{R_g T}\left(E - E^{0\prime}\right)} - C_O^* e^{-\frac{\alpha nF}{R_g T}\left(E - E^{0\prime}\right)} \right]}{1 + \frac{k_0}{m_O} \left[e^{\frac{(1-\alpha)nF}{R_g T}\left(E - E^{0\prime}\right)} + e^{-\frac{\alpha nF}{R_g T}\left(E - E^{0\prime}\right)} \right]} \quad \textbf{(S.18)}$$

Substituting I_{ss} in equations (**S.14**) and (**S.15**) finally allows obtaining surface concentrations as a function of bulk concentrations, mass transfer coefficient and charge transfer kinetic constant:

$$C_R^s = \frac{C_R^* + (C_R^* + C_O^*) \frac{k^0}{m_O} e^{-\frac{\alpha nF}{R_g T}\left(E - E^{0\prime}\right)}}{1 + \frac{k^0}{m_O} \left[e^{-\frac{\alpha nF}{R_g T}\left(E - E^{0\prime}\right)} + e^{\frac{(1-\alpha)nF}{R_g T}\left(E - E^{0\prime}\right)} \right]} \quad \textbf{(S.19)}$$

$$C_O^s = \frac{C_O^* + (C_R^* + C_O^*) \frac{k_0}{m_O} e^{\frac{(1-\alpha)nF}{R_g T}\left(E - E^{0\prime}\right)}}{1 + \frac{k_0}{m_O} \left[e^{-\frac{\alpha nF}{R_g T}\left(E - E^{0\prime}\right)} + e^{\frac{(1-\alpha)nF}{R_g T}\left(E - E^{0\prime}\right)} \right]} \quad \textbf{(S.20)}$$